

© 2016 IEEE. Personal use of this material is permitted. Permission from IEEE must be obtained for all other uses, in any current or future media, including reprinting/republishing this material for advertising or promotional purposes, creating new collective works, for resale or redistribution to servers or lists, or reuse of any copyrighted component of this work in other works. Access to this work was provided by the University of Maryland, Baltimore County (UMBC) ScholarWorks@UMBC digital repository on the Maryland Shared Open Access (MD-SOAR) platform.

Please provide feedback Please support the ScholarWorks@UMBC repository by emailing scholarworks-group@umbc.edu and telling us what having access to this work means to you and why it's important to you. Thank you.

Whole-brain data-driven approaches for capturing and characterizing time-varying spatio-temporal brain connectivity in fMRI data

Vince D Calhoun^{1,2} and Tülay Adalı³

¹*The Mind Research Network & LBERI, Albuquerque, New Mexico.*

²*Dept. of ECE, University of New Mexico, Albuquerque, New Mexico*

³*Dept. of CSEE, University of Maryland, Baltimore County, Baltimore, MD*

IEEE Signal Processing Magazine
Printed: 28 March 2021

Correspondence:

Vince Calhoun, Ph.D.
The Mind Research Network
1101 Yale Blvd NE
Albuquerque, NM 87106
Phone: 505 272-1817
E-mail: vcalhoun@unm.edu

Abstract:

The study of whole-brain functional brain connectivity with functional magnetic resonance imaging (fMRI) has been largely based on the assumption that a given condition (e.g., rest or task) can be evaluated by averaging over the entire experiment. In actuality, the data are much more dynamic, showing evidence of time-varying connectivity patterns, even within the same experimental condition. In this paper, we review a family of blind-source separation (BSS) approaches that have proven useful for studying time-varying patterns of connectivity across the whole brain. Initial work in this direction focused on time varying coupling among data-driven nodes, but more recently time-varying nodes have also been considered. We also discuss extensions of these approaches including transformations into the time-frequency domain and others. We also provide a rich set of examples of various applications that yielded new information about the healthy and the diseased brain. In sum, due in large part to developments in the field of signal processing, the fMRI community has seen a major new development in the development of approaches that can both capture whole-brain systemic connectivity information (connectomics) while also allowing this system to evolve over time as it naturally does (i.e., chronnectomics).

Keywords: connectome, chronnectome, dynamics, connectivity, brain function, independent component analysis

Introduction

Big data¹, the human connectome², the BRAIN initiative³, and the chronnectome⁴: There is a major ongoing movement in the US, European Union, China, and Japan to understand the human brain and brain connectivity (cf. human connectome project^{2,3} and BRAIN initiative (multi-agency), NSF's neural & cognitive systems program, the Human Brain Project (EU), Brain/MINDS (Japan), and others). Critical themes across all of these projects are technology development for studying the human brain and harnessing developments resulting from the human genome project and others. These themes continue to revolutionize our understanding of the complexity of the human brain, and are driving the recent focus on scaling science to handle “big data” problems. The study of changes in brain networks (functional connectomics^{5,6}) over time, termed the ‘chronnectome’, was recently highlighted as one of the “Best of 2014” by NIMH Director Dr. Tom Insel⁷ in terms of a concept that brought engineers, physicists, and neurobiologists together to better understand the temporal dynamics of the brain imaging signals. Specifically, Dr. Insel noted the power of “convergence” or merger of multiple disciplines^{7,8}. The chronnectome is a model of the brain in which nodal activity and connectivity patterns are changing in predictable and meaningful ways through time^{4,9}. Thus, the concept of the chronnectome, is making the specific assumption that the dynamics are nonstationary in interesting ways. One can focus on chronnectomic changes at various scales, including milliseconds (as measured by EEG or MEG), seconds (as measured by fMRI), minutes (as measured by changes between experiments using average or static connectivity approaches¹⁰⁻¹²), and changes over months/years (at which point incorporating additional information such as changes in brain structure or epigenetic changes becomes very useful for longitudinal studies) (see **Figure 1a**). Characterization of brain connectivity across the lifespan is a major priority both in the human connectome project⁵ and the BRAIN initiative³.

Figure 1: (a) The Chronnectome concept of studying connectivity at multiple time scales⁴, (b) overview of some of the key steps and options used in computing time-varying connectivity measures.

One of the earliest examples of time-varying connectivity is the concept of EEG microstates, or points in time during which there is a common synchrony across multiple brain regions¹³⁻¹⁷. More recently, fMRI, which provide a more spatially specific measure of function across the entire brain (at the cost of decreased temporal resolution), has been used to study time-varying connectivity. In this review, we primarily focus on the recent emergence of data-driven approaches that can capture whole-brain patterns of time-varying connectivity within one fMRI experiment (either at rest or during a task). Initial results suggest that such an approach provides more information than static connectivity approaches, thus motivating methods that acknowledge the dynamically changing brain within a single experiment. Such approaches will likely make evaluation of connectivity changes over longer time scales even more informative. There has been great progress in the use of functional connectivity measures to study the healthy and diseased brain, and whole-brain measures have proven extremely powerful. The functional magnetic resonance imaging (fMRI) community has now realized that assessment of functional connectivity has been limited by an implicit assumption of spatial and temporal stationarity throughout the measurement period¹⁸. Dynamics are potentially even more prominent in the resting-state, during which mental activity is unconstrained¹⁹. The development or adaptation of approaches to study time-varying connectivity in the brain has emerged along multiple lines, including the detection of important transition points (e.g. changepoint analysis²⁰), time-frequency approaches²¹, and windowing approaches²²⁻²⁴.

Data-driven approaches, in particular (joint) blind source separation has proven useful for taking advantage of the available prior and statistical information to fully characterize both static and dynamic brain connectivity^{25,26}. Hence, the term chronnectome describes a focus on

identifying time-varying, but *reoccurring*, patterns of coupling among brain regions. The chronnectome (in contrast to another interesting concept called the dynome, which is focused on time-varying (oscillatory) activity whose basic characteristics (frequency, phase, amplitude, etc.) are generally assumed to be static²⁷) is making the specific assumption that the dynamics are nonstationary in interesting ways. In the context of this paper, ‘dynamics’ is thus referring to intrinsic nonstationarities rather than dynamics in its mathematical sense. A number of approaches in this respect are revealing exciting new information about the brain including information about sleep states²⁸ as well as disease²⁹, and represent a much more natural way to analyze brain imaging data, especially that which is largely unconstrained, such as resting fMRI data. A high-level summary of the key steps for capturing whole-brain data-driven time-varying connectivity is presented in **Figure 1b**. Input to the analysis can consist of timecourses from regions or from networks (e.g. component timecourses). Next, timecourse pairs can be analyzed using a fixed or adaptive windowing approach^{23,30} or a time-frequency approach^{21,31}. The next step involves estimating the states, which can be done a number of ways, e.g. k-means clustering³⁰, PCA^{26,32} or ICA^{33,34}. Finally, summary measure of the states can be done for each state separately, e.g. dwell time or connectivity within each state matrix^{29,35}, or across all states such as in a meta-state approach^{33,34}.

In the remainder of this article, we highlight some key signal-processing aspects of the ongoing chronnectomics work with a focus on whole-brain data-driven approaches applied to fMRI data. We start by introducing approaches for defining the input features that are used in such approaches, with a particular focus on data-driven approaches that can help estimate time-varying aspects of both the functional connectivity and the spatial locations. Next, we introduce static and dynamic connectivity and discuss a number of relevant issues including validation. We then provide several examples of the many current applications that have emerged based on blind source separation-based methods developed in our lab. In contrast to previous

reviews^{4,18}, the focus of the current article is to review data-driven whole-brain approaches from a signal processing perspective. In addition, we offer new high-level summaries of the various steps in capturing time-varying connectivity (**Figure 1b**), new approaches (e.g. whole-brain time-frequency analyses), new strategies for modeling (e.g. subspace analysis and dynamic model-based connectivity) and new application examples (e.g. results from the EEG/fMRI sleep study and the substance use study).

Feature generation

One key challenge for studying time-varying connectivity in the brain is generating the features that capture the time-varying dynamics. Approaches include those that make use of a priori information, e.g., picking a pair of brain regions (seeds) or using a whole-brain predefined atlas of regions in fMRI data as well as data-driven approaches. Data-driven approaches include sparsity-based parcellation³⁶ and latent variables analysis methods such as principal component analysis (PCA), group independent component analysis (ICA)³⁷ spatially constrained ICA³⁸, independent vector analysis²⁵, and tensor decompositions³⁹. For example, in^{40,41} first event related potentials in EEG data are detected and then summarized using PCA of time-dependent node correlation matrices. On the other hand, for fMRI data, decompositions that use ICA and IVA can be adapted to extract dynamic features in multiple ways as demonstrated in^{30,34,42} among other references.

Independent component analysis: ICA is based on the assumption that the observations are a linearly mixed set of independent sources/components, an assumption that allows identification of the original sources subject to only scaling and permutation ambiguities, and under rather mild conditions for identifiability. If we consider the simple linear mixing model $\mathbf{x}(v) = \mathbf{A}\mathbf{s}(v)$, $1 \leq v \leq V$, $\mathbf{x}(v), \mathbf{s}(v) \in \mathcal{R}^N$ where v is the sample index such as voxel, pixel, or time and the mixing matrix \mathbf{A} is full rank, one can obtain the independent component

estimates $\mathbf{u}(v) = \mathbf{W}\mathbf{x}(v)$ by estimating a demixing matrix \mathbf{W} through optimization of an appropriate cost measuring independence^{25,43}.

ICA has proven very useful for fMRI data analysis, and can be performed in two different ways^{44,45} namely spatial ICA that extracts independent spatial maps, and temporal ICA that extracts independent time courses by considering the transposed version of the data matrix. Spatial ICA is more widely used as the spatial independence assumption is better suited for the systematically non-overlapping nature of the spatial patterns⁴⁶. For spatial ICA, the data matrix \mathbf{X} is formed by flattening a given slice at time t as a row such that \mathbf{X} is time points by voxels, $T \times V$, and dimension T is typically reduced to N using PCA prior to ICA.

In the group ICA model^{37,47}, which has been implemented in the GIFT toolbox (available at <http://mialab.mrn.org/software/gift>), there are double dimension reduction stages using PCA where the first step is to perform a subject level PCA, and after vertical concatenation of dimension-reduced subject data, a second level PCA is applied at the group level to estimate a common group subspace⁴⁸. Individual subject maps are then reconstructed using the group and subject-level PCA matrices thus preserving most of the variability for individual subjects. Other implementations and uses of the Group ICA model are also possible and discussed in³⁷. An example of the traditional use of group ICA is shown in **Figure 2**. The spatial maps are characterized by a single timecourse and provide information about the degree to which each voxel is linearly related to that timecourse, as such it informs us about within network connectivity. In the figure components are divided into anatomical domains (each box is a domain) and within a domain different components are indicated with different colors. Relationships among the timecourses (matrix in **Figure 2**) capture the functional network connectivity or among-network connectivity. The matrix indicates the degree to which each component is correlated with the other components. Correlations are positive (red) values and anticorrelations (blue) are represented as negative values. Results are shown for healthy

controls (HC) and patients with schizophrenia (SZ)²⁹. Some approaches have also attempted to combine aspects of both spatial and temporal ICA^{44,49}.

Figure 2: Data-driven maps from group ICA provides components that capture information about within network (component) connectivity that are characterized by timecourses that can be used to assess functional network connectivity (FNC) or among network connectivity which can be assessed in the simplest manner by computing the cross-correlation among component timecourses. Results are shown for healthy controls (HC) and patients with schizophrenia (SZ)²⁹.

Independent vector analysis: In independent vector analysis (IVA), one explicitly assumes a separate source and mixing matrix for each dataset and, for K datasets, write $\mathbf{x}^{[k]}(v) = \mathbf{A}^{[k]}\mathbf{s}^{[k]}(v)$, $\mathbf{x}^{[k]}(v), \mathbf{s}^{[k]}(v) \in \mathcal{R}^N$ $k = 1, 2, \dots, K$. Then the independent decomposition of all K datasets is achieved jointly by fully taking advantage of the statistical second and higher-order correlation that exist among the datasets.

The key definition in the formulation of IVA is the source component vector (SCV) that is formed by using the corresponding elements of the source random vectors $\mathbf{s}^{[k]}(v)$ such that the n th SCV is given by $[s_n^{[1]} s_n^{[2]}, \dots, s_n^{[K]}]^T$ where the subscript refers to n th source in each of K datasets, e.g., for data from K subjects, this would be the n th spatial map for each subject^{25,50}. The IVA decomposition is achieved by minimizing the mutual information among the SCVs (as opposed to sources in ICA) which is equivalent to finding sources that are independent within each dataset while maximizing the mutual information within each one of N SCVs²⁵. The use of this statistical dependence allows the mitigation of permutation ambiguity for sources (modes) that are dependent across the datasets, so that the source estimates across subjects are aligned.

Capturing time-varying connectivity

The capture of time-varying coupling between variables is a topic which has been heavily studied in other fields and in communications for signal processing in particular. However, the specific application to whole-brain functional connectivity is relatively new²² and its application to brain imaging data poses particular challenges that are currently being studied. One important challenge is how to best identify relevant features from the high-dimensional brain imaging data. Both group ICA and IVA can be effectively used for extracting features of interest from the fMRI data that in a second step can be used to characterize the dynamic properties. In this section, we provide a brief introduction of the use of both tools in this context.

Time-varying connectivity captured with group ICA: One approach is to use group ICA of multiple subjects and after selection of components of interest, capturing time-varying changes in the coupling (e.g. covariance) among component timecourses, using FNC with a tapered window³⁰. The FNC information shown in **Figure 2** was computed by assuming the connectivity is static throughout the experiment. Dynamic approaches capture time-varying connectivity within fMRI data^{30,51} or changes in the spatial maps (spatial FNC). The simplest approach is to use a windowing method^{24,30,52}. An example of this can be seen in **Figure 3** in which group ICA was run on multiple subjects, followed by selection of components of interest and then cross-correlation of the ICA time courses, called dynamic FNC (dFNC). On the left side is shown a cross-correlation matrix for the entire ICA timecourse for a single subject. A tapered Gaussian window was used to compute time-varying correlation matrices (top of **Figure 3-A2**, with individual correlations shown at the bottom of A2 for the black boxes marked in the matrix in A1). There is considerable variability in the connectivity, which does not appear to be noise due to the modularity of the correlation matrices and the fact that the time course tends to be low frequency.

Figure 3: FNC dynamics via windowing: single example subject: (A1) average FNC (cross-correlation of ICA time courses) for a single subject, (A2) FNC time series between select components and snapshots of whole-brain FC³⁰.

Dynamics of spatial patterns captured with IVA: We can also process overlapping windows jointly using IVA as demonstrated in ⁴² to capture time-varying spatial patterns. Since IVA jointly optimizes independence, use of shorter time windows becomes possible allowing for sufficient statistical power for the estimation. One example for the use of IVA to capture changes in the spatial coupling (either changes in the within component maps or in the coupling among spatial networks) is to use it in conjunction with a group level PCA⁴⁸. The data are partitioned into K time windows of equal size T , and then the window from each of the M subjects is analyzed groupwise as shown in **Figure 4**. In the figure, the dimensionality of each dataset \mathbf{X} is reduced from MT to N , resulting in dimension reduced datasets. This approach enables us to capture changes in the spatial patterns reflecting connectivity over time. We show later summary of results from an application of this approach to evaluate group differences in spatial dynamics.

Figure 4: Independent vector analysis approach to characterize spatially dynamic and static components^{4,18,42}. Here spatial maps of a component vector are related over the time windows but should be distinct from the spatial maps of all other components (whether within or outside the current window w_i).

Characterization of time-varying connectivity

Once the relevant features are extracted from the data, they must be analyzed to evaluate their dynamic properties. Here, we briefly mention three important approaches among those: Markov modeling, meta-states analysis based on windowed or adaptive approaches (e.g., where pairwise correlations are computed using small portions of the data), and time-frequency

analysis (where a time-frequency approach is used to transform the data and study patterns of amplitude, phase, and frequency over time^{21,31}).

Markov modeling/state transitions: Markov chain modeling provides a powerful way to characterize (and hence distinguish) time-varying connectivity^{30,42}. A data-driven approach can be used to learn both the states and the transitions from the data (in both space and time).

Figure 5A shows the state assignments as a function of time for three example subjects for the dFNC approach. Transition behavior can be characterized by considering a Markov chain (MC) in which the probability to go from the current state to the next state is conditionally independent from all states that occurred (in time) before the current state. In **Figure 5B**, we show the average transition matrix (TM) for our example. Red squares along the diagonal signify a very high probability of staying in the same state. For the off-diagonal elements, hotter colors in the S1 column indicate a higher probability of entering S1 from the other states, and cooler colors in the S3 row indicate a lower probability of exiting S3. Because the MC is irreducible (any state can be reached from any other state in a finite number of steps), its stationary distribution (π) can be obtained as the principal eigenvector of the estimated TM⁵³. The vector π , displayed in **Figure 5C**, represents the probability distribution over the states of the MC when the chain is in its stationary regime, i.e., in the expected behavior of the system in the long-run. In our example, the stationary probability for S3 is far greater than the probabilities for other states, meaning that in the long-run the system is most likely to be found in S3. Markov chains enable us to capture the propagation of probability distribution vectors over the states (i.e., mixed state vectors) through a network.

Figure 5: A) State vectors for the three example subjects. Assigned states are plotted at the time point corresponding to the center of the sliding window. (B) The state transition matrix (TM), averaged over subjects. High values along the diagonal indicate a high probability of staying in a state. Note that transition probability is color-mapped on a log-scale. (C) The stationary probability vector (π , principal eigenvector of the TM) shows the steady-state, or “long-run” behavior. Error bars indicate the non-parametric 95%

confidence intervals (CIs) obtained from 1000 bootstrap resamples of the average TM (resampling subjects).

Cross-state summary measures (e.g. meta-states): A core challenge for dynamic network connectivity analysis is to summarize the data in ways that simultaneously reduce its dimensionality and expose features that are strongly predictive of important population characteristics. The native dimension of network correlation space can easily exceed 1000. However recent approaches have been developed to summarize the dynamic information in a higher level summary. In this case, the goal is to calculate a tractable characterization of time-varying connectivity in terms of the additive contributions of a set of basis correlation patterns (BCPs) obtained according to some specified optimization criterion (using, for example, temporal ICA, spatial ICA, PCA or k-means clustering)^{34,54}. A BCP in the context of a PCA-based approach would be called an eigenconnectivity. This is summarized in the “Estimation of dynamic states” panel of **Figure 1b**. The time-indexed N -element vectors of BCP weights, discretized according to signed quartile, are the meta-states. In a recent work (see **Figure 6**), results showed a summary of a 3-level 5-state quantization in 400 healthy subjects that indicates 1) only 22 of these meta-states are occupied more than 1% of the time, 2) these states including mostly single or double state occupancy, and 3) females show more single state occupancy than males, who show more double state occupancy³⁴. Using a large, balanced multi-site dataset, we have also investigated the effect of SZ diagnosis on four interrelated measures of meta-state dynamism, separately evaluated with respect to BCPs obtained from four common algorithms⁵⁵. These analyses have yielded consistent and significant evidence for reduced connectivity dynamism in schizophrenia patients and provide strong evidence in support of such summary measures. There are a number of possible ways to compute cross-state summary measures, a topic of ongoing work. One example of such a metrics is the concept of a k-level hub (e.g. states that are returned to k or more times). Related concepts include absorbing

(subjects stay for extended periods of time) and transient (subjects come in and out multiple short periods of time) hubs, both of which appear highly different in schizophrenia⁵⁵.

Figure 6: Bar chart shows relative occurrence frequency of each combo-state. The bottom label of each bar is the coded and visual representation of the associated combo-state and the top is labeled by the gender that on average occupies that combo-state more along with the FDR-adjusted p-values for that comparison (dark blue: M>F and dark red: F>M). On the top right corner of the figure, each of the pie chart shows overall occurrence frequency of the associated combo-state³⁴.

Time-frequency analysis: Chang et al. first introduced the use of time-frequency methods to study time-varying connectivity (coherence) in a few regions of interest²¹. More recently, a whole-brain time frequency approach was proposed that enables brain states to be estimated. The proposed approach can be considered an extension and generalization of both the time-domain³⁰ and the coherence approaches²¹ (see ⁵⁶ for more details). Using this approach, we can more fully characterize a state via multiple frequency bands by its connectivity pattern (covariance), frequency contribution, and phase (e.g., anticorrelated pairs would have a 180 degree phase shift). **Figure 7** shows an example of a state that was defined via k-means clustering after the use of a complex Morlet filter to separate 5 different frequency bands with magnitude and phase. This particular state has most of its power within 0.07-0.13 Hz, has some strong 0 and 180 degree phase patterns, and captures some very interesting patterns. Results from a large rest fMRI dataset ($N=400$) identified two states, with similar correlation patterns, but distinct frequency profiles, one of which was highly predictive of males versus females³¹. This provides additional evidence that ignoring the dynamic information obscures important information.

Figure 7: Multiband state with 25% occurrence rate showing the most power in the 0.07 and 0.13 frequency bands. Phase histogram and color indicate the phase of the dynamics.

Validation

There have been quite a few studies published that provide important information validating the presence of chronnectomic information in fMRI data. For example, one study of a large $N = 400$ subject dataset performed a split-half replication and also varied a number of parameters including the number of estimated states and the window size⁵⁷. Other studies have shown that dynamic connectivity tracks closely with sleep state²⁸, psychedelic experience⁵⁸, are reflected in both humans and macaques⁵¹, and are associated with daydreaming⁵⁹. Cross-validated classification also appears to be more powerful when applied to dynamic connectivity measures^{4,60}. The comparison of dynamic connectivity measures in the presence of tasks which activate known brain regions also provides powerful evidence to support the presence of connectivity states^{18,61}.

Concurrent EEG/fMRI Experiments: Concurrent EEG provides a useful way to validate these dynamic changes by providing convergent evidence for them. While EEG alone cannot provide a ground truth measure, since EEG and fMRI are generated by and sensitive to very different sources, we do expect that fMRI changes in connectivity over time that reflect neuronal changes will also be detectable with EEG. An illustrative example focused on differences in dynamics associated with the eyes open versus eyes closed state is presented in **Figure 8**. Concurrent EEG/fMRI data are collected using a Brain Products EEG system, which had been previously used to collect data comparing a variety of frequencies in EEG with fMRI data in the resting state for eyes open and eyes closed^{62,63}. Preliminary analysis of these data using a group ICA approach to evaluate temporal dynamics is shown in **Figure 8**⁶⁴. The left panel shows two dynamic states estimated from the fMRI data. Both of these states showed a significant difference with eyes open vs closed with S1 being dominantly occurring for eyes open, whereas S5 showing significantly more occurrence during the eyes closed stage and demonstrating more EEG alpha power. The anti-correlation with brain regions associated with

inner reflection (regions in the widely studied default mode network⁶⁵) was also stronger in the eyes open data, and as the states were associated with more EEG drowsiness measures, these anti-correlations diminished and then subsided⁶⁴. This is only a relatively simple approach to relating EEG and fMRI data, more advanced methods that take advantage of the joint information during the estimation process would likely be even more fruitful in demonstrating the benefits of dynamic connectivity^{63,66-69}.

Figure 8: Concurrent EEG/fMRI temporal dynamics during eyes open (EO) versus eyes closed (EC)⁶⁴. fMRI analysis on the left, and EEG data analyzed within identified fMRI states for one electrode shown on the right top panel. EEG data reflected considerably more theta/delta power during the states occurring more in the EC condition. EEG was strongly correlated with the identified fMRI states as show in the panel on bottom right showing the distance among EEG and fMRI which reduced as EEG windows were shifted in time away from the fMRI states.

Incorporating dynamics improves contrast-to-noise: Data shown in **Figure 9** were evaluated from a normative resting fMRI data set ($N=200$ healthy controls) using a simple model that incorporates an explicit static subspace (while modeling the dynamic information in a nuisance subspace). In this case, the model that incorporates the dynamic information (**Figure 9** right) shows a higher contrast-to-noise ratio than when the dynamic information is completely ignored (**Figure 9** left). This result also provides strong support for the use of models that capture both the static and dynamic connectivity information.

Figure 9: Data showing static FNC pattern estimated by a model incorporating dynamics has higher contrast-to-noise than one ignoring dynamics.

Choice of estimation strategy and parameters: One common critique of windowed correlation approaches is that they can introduce spurious correlations^{24,70}. There have been a number of papers that evaluate various window parameters and performance in simulations in real data quite carefully^{22,24,30}. In particular spurious changes in connectivity appear if the

Running head: Time-varying brain connectivity

sliding window length is shorter than the largest period present in the signals²⁴, suggesting window lengths of at least 30 seconds for fMRI. The combination of multimodal data (e.g. EEG and fMRI) might help mitigate the issue and confirm that the changes are real⁷¹. Instead of a fixed window, adaptive windowing approaches can also be used²³. More importantly, fixed windowed approaches perform quite similarly in their mean to adaptive windowing approaches²³. In addition, the combination of multivariate approaches with windowing appears to be more robust to spurious correlations than univariate approaches⁴. Another choice involved is the number of states. This has not yet been evaluated comprehensively, though in multiple papers, an evaluation of results with various numbers of states is presented in order to ensure that results are not heavily dependent on the final choice (see, e.g. ³⁰).

Applications

There have already been numerous uses of time-varying connectivity in fMRI data. In this section, we review three interesting applications: first, a study of changes in spatial connectivity patterns in schizophrenia, second, an evaluation of the relationship between sleep stage and connectivity, and finally, an evaluation of the differences in connectivity states in individuals who are either heavy smokers or heavy drinkers.

Changes in time-varying spatial patterns in schizophrenia patients: It is challenging to consider changes over time in both spatial and temporal aspects of connectivity, but spatial patterns are also an important aspect of the dynamic information. In an analysis of patients with schizophrenia and healthy controls, we use the windowed IVA approach shown in **Figure 4** with 7 windows each of which overlapped by 50% to cover a 200 timepoint resting fMRI data set. Thirty components were estimated, 12 of them were determined to be related to brain function and not artifact. It is shown, through computation of Markov chain transition probabilities between multiple states, that controls show significantly less probability to transition between states. This provides a way to summarize changes in the spatial patterns

over time. We can also evaluate changes in the dependencies between pairs of spatial networks over time. To estimate spatial dependencies we can compute a mutual information matrix for each subject and each window. The spatiotemporal dependency dynamics are very interesting and some show significant differences between schizophrenia and healthy controls (e.g. schizophrenia patients show more coupling between medial prefrontal cortex (brain regions thought to mediate cognition) and temporal lobe (regions which process sound and language and are known to be disrupted in schizophrenia) network dynamics than controls, **Figure 10**). This is a simple summary measure of only 7 windows but it indicates that spatial dynamics are a sensitive measure of disease state.

Figure 10: Schizophrenia patients exhibit significant changes in the spatial dependency between default mode and temporal lobe networks.

Time-varying connectivity in fMRI maps to EEG defined sleep stages: As evidence of the utility of the dynamic patterns, we evaluated resting state fMRI data collected from 55 subjects for 50 minutes each (1500 volumes, TR=2.08 s) with a Siemens 3T Trio scanner while the subjects transitioned from wakefulness to at most sleep stage N3 (details in ⁷²). Simultaneous EEG was acquired facilitating sleep staging according to AASM criteria resulting in a hypnogram per subject (a vector assignment of consecutive 30s EEG epochs to one of awake, N1, N2 and N3 sleep). Following our recent work³⁰, we estimated dFNC between components following a group ICA. We then computed the counts of these dFNC windows for each hypnogram state. Results show states 1 and 5 map strongly onto the awake and deeper sleep stages, respectively (see **Figure 11**)⁷³. More work is needed, but results strongly support the utility of capturing dynamic connectivity.

Figure 11: Dynamic states 1 and 5 map onto awake and deeper sleep stages.

Time-varying connectivity is significantly changed in substance users: A greater understanding of individual differences in the neurobiology of substance use is integral to developing more effective interventions. A large body of evidence shows aberrant brain structure and function in substance users. While some specific regions are implicated (e.g. mesocorticolimbic regions) in craving and loss of controls, for the most part, these studies are heterogeneous and do not provide the ability to discriminate between substance users and controls at the level of the individual. In part we believe this is because the connectivity methods have focused on static measures and hence did not fully capture the variability of the patterns within the patient groups. In particular, it is clear that 1) large heterogeneity in the SUD brain function makes analysis challenging, 2) while certain brain pathways have been hypothesized as most affected, all of these disorders encompass multiple interacting brain regions. Hence being able to evaluate the dependencies between multiple functional brain networks is critical to understand the disorders. dFNC results were computed for smokers and drinkers ($N=50$) and identified significant changes in correlation among multiple brain networks.

In **Figure 12**, dFNC matrices for two dynamic states showing differences among smokers and drinkers are shown. State 1 lacks most of the anticorrelation between default mode and other networks (pink boxes), as well as the connectivity within sensorimotor regions. Some interesting differences are also apparent when evaluating the dwell time each group spent in the dynamic states. For example, smokers and drinkers both spent significantly more of their time within state 2. The percent time each group spend in these two states is illustrated in **Figure 13** and is significantly different between controls, smokers, and drinkers. Neither of these interesting results is observable from the static results. The importance of such a result, is that the ability of methods that focus on dynamics to separate out information about the neurobiology of substance use may teach us more about how the brain is different in nicotine

or alcohol use, and importantly this information may provide a more accurate biomarker that can be used to predict, e.g. treatment outcomes.

Figure 12: Dynamic FNC ‘states’ that showed significant group differences. In particular, smoker and drinker spent more time in State 1 vs State 2 (of 5 estimated states). Notably, state 1 lacks the predominant anticorrelation between default mode regions which is visible in state 2 suggesting their lack may serve as either a protective factor or as a marker of substance use.

Figure 13: Dwell time (percent) for states 1 and 2. Smoker and drinkers are spending significantly ($p < 0.0001$) more time in state one whereas controls are spending more of their time in state 2.

Conclusions

In summary, time-varying connectivity is a powerful tool for improving our understanding of the brain. There are still plenty of avenues of ongoing investigation that require creative thinking and the development of advanced signal processing methods to improve the estimation performance and the extraction and characterization of meaningful information. For example, some specific directions of interest include the development of approaches that can capture both static and dynamic connectivity patterns. Also, approaches that can capture spatiotemporal patterns of connectivity would be very desirable as it is clear that both are changing in systematic and interesting ways. Finally, more studies that map task information onto the states will help our understanding of the function of these connectivity states⁷⁴. Finally, there is important need for continued work in characterizing single-states, multiple-states, or other summary measures that provide intuitive ways of conveying brain connectivity in a way that respects the dynamic nature of the brain. Such approaches should inform us about the healthy brain as well as point us to important aspects of disease, especially for complex mental illnesses such as schizophrenia and autism spectrum disorder.

Acknowledgements

We would like to thank Victor Vergara, Robyn Miller, Maziar Yaesoubi and Eswar Damaraju for their input and help with data processing. The work was in part funded by NIH via a COBRE grant P20GM103472 and grants R01EB005846 and 1R01EB006841.

References

- [1] N. B. Turk-Browne, "Functional interactions as big data in the human brain," *Science*, vol. 342, pp. 580-584, Nov 1 2013, 3970973.
- [2] D. C. Van Essen, K. Ugurbil, E. Auerbach, D. Barch, T. E. Behrens, R. Bucholz, A. Chang, L. Chen, M. Corbetta, S. W. Curtiss, S. Della Penna, D. Feinberg, M. F. Glasser, N. Harel, A. C. Heath, L. Larson-Prior, D. Marcus, G. Michalareas, S. Moeller, R. Oostenveld, S. E. Petersen, F. Prior, B. L. Schlaggar, S. M. Smith, A. Z. Snyder, J. Xu, E. Yacoub, and W. U.-M. H. Consortium, "The Human Connectome Project: a data acquisition perspective," *Neuroimage*, vol. 62, pp. 2222-2231, Oct 1 2012, 3606888.
- [3] P. S. Weiss, "President Obama announces the BRAIN Initiative," *ACS Nano*, vol. 7, pp. 2873-2874, Apr 23 2013.
- [4] V. D. Calhoun, R. Miller, G. D. Pearlson, and T. Adalı, "The chronnectome: Time-varying connectivity networks as the next frontier in fMRI data discovery," *Neuron*, vol. 84, pp. 262-274, 2014, PMC Journal - In Process.
- [5] D. C. Van Essen, S. M. Smith, D. M. Barch, T. E. Behrens, E. Yacoub, K. Ugurbil, and W. U.-M. H. Consortium, "The WU-Minn Human Connectome Project: an overview," *Neuroimage*, vol. 80, pp. 62-79, Oct 15 2013, 3724347.
- [6] R. C. Craddock, S. Jbabdi, C. G. Yan, J. T. Vogelstein, F. X. Castellanos, A. Di Martino, C. Kelly, K. Heberlein, S. Colcombe, and M. P. Milham, "Imaging human connectomes at the macroscale," *Nat Methods*, vol. 10, pp. 524-539, Jun 2013.
- [7] T. Insel, Director's Blog: Best of 2014, <http://www.nimh.nih.gov/about/director/2014/best-of-2014.shtml>.
- [8] P. A. Sharp and R. Langer, "Research agenda. Promoting convergence in biomedical science," *Science*, vol. 333, p. 527, Jul 29 2011.
- [9] R. F. Betzel, L. Byrge, Y. He, J. Goni, X. N. Zuo, and O. Sporns, "Changes in structural and functional connectivity among resting-state networks across the human lifespan," *Neuroimage*, vol. 102 Pt 2, pp. 345-357, Nov 15 2014.
- [10] M. J. Brookes, J. R. Hale, J. M. Zumer, C. M. Stevenson, S. T. Francis, G. R. Barnes, J. P. Owen, P. G. Morris, and S. S. Nagarajan, "Measuring functional connectivity using MEG: methodology and comparison with fcMRI," *Neuroimage*, vol. 56, pp. 1082-1104, Jun 1 2011, 3224862.
- [11] M. J. Brookes, M. Woolrich, H. Luckhoo, D. Price, J. R. Hale, M. C. Stephenson, G. R. Barnes, S. M. Smith, and P. G. Morris, "Investigating the electrophysiological basis of resting state networks using magnetoencephalography," *Proc Natl Acad Sci U S A*, vol. 108, pp. 16783-16788, Oct 4 2011, 3189080.
- [12] J. M. Houck, M. Cetin, A. Mayer, J. Bustillo, M. Brookes, and V. D. Calhoun, "Comparison of resting intrinsic connectivity networks in schizophrenia and healthy controls computed via group spatial ICA of MEG and fMRI data," in *Proceedings of the Organization of Human Brain Mapping*, Hamburg, Germany, 2014.
- [13] R. D. Pascual-Marqui, C. M. Michel, and D. Lehmann, "Segmentation of brain electrical activity into microstates: model estimation and validation," *IEEE Trans Biomed Eng*, vol. 42, pp. 658-665, Jul 1995.
- [14] T. Koenig, L. Prichep, D. Lehmann, P. V. Sosa, E. Braeker, H. Kleinlogel, R. Isenhardt, and E. R. John, "Millisecond by millisecond, year by year: normative EEG microstates and developmental stages," *Neuroimage*, vol. 16, pp. 41-48, May 2002.
- [15] J. Kindler, D. Hubl, W. K. Strik, T. Dierks, and T. Koenig, "Resting-state EEG in schizophrenia: auditory verbal hallucinations are related to shortening of specific microstates," *Clin Neurophysiol*, vol. 122, pp. 1179-1182, Jun 2011.

- [16] D. Lehmann, "Topography of spontaneous alpha EEG fields in humans," *Electroencephalogr Clin Neurophysiol*, vol. 30, pp. 161-162, Feb 1971.
- [17] D. Lehmann, H. Ozaki, and I. Pal, "EEG alpha map series: brain micro-states by space-oriented adaptive segmentation," *Electroencephalogr.Clin.Neurophysiol.*, vol. 67, pp. 271-288, 1987.
- [18] R. M. Hutchison, T. Womelsdorf, E. A. Allen, P. Bandettini, V. D. Calhoun, M. Corbetta, S. D. Penna, J. Duyn, G. Glover, J. Gonzalez-Castillo, D. A. Handwerker, S. D. Keilholz, V. Kiviniemi, D. A. Leopold, F. de Pasquale, O. Sporns, M. Walter, and C. Chang, "Dynamic functional connectivity: promises, issues, and interpretations," *NeuroImage*, vol. 80, pp. 360-378, 2013, PMC3807588.
- [19] Z. Shehzad, A. M. Kelly, P. T. Reiss, D. G. Gee, K. Gotimer, L. Q. Uddin, S. H. Lee, D. S. Margulies, A. K. Roy, B. B. Biswal, E. Petkova, F. X. Castellanos, and M. P. Milham, "The Resting Brain: Unconstrained yet Reliable," *Cerebral Cortex*, Feb 16 2009.
- [20] I. Cribben, R. Haraldsdottir, L. Y. Atlas, T. D. Wager, and M. A. Lindquist, "Dynamic connectivity regression: determining state-related changes in brain connectivity," *Neuroimage*, vol. 61, pp. 907-920, Jul 16 2012.
- [21] C. Chang and G. H. Glover, "Time-frequency dynamics of resting-state brain connectivity measured with fMRI," *Neuroimage*, vol. 50, pp. 81-98, Mar 2010, 2827259.
- [22] U. Sakoglu, G. D. Pearlson, K. A. Kiehl, Y. M. Wang, A. M. Michael, and V. D. Calhoun, "A method for evaluating dynamic functional network connectivity and task-modulation: application to schizophrenia," *MAGMA*, vol. 23, pp. 351-366, Dec 2010, 2891285.
- [23] M. A. Lindquist, Y. Xu, M. B. Nebel, and B. S. Caffo, "Evaluating dynamic bivariate correlations in resting-state fMRI: A comparison study and a new approach," *Neuroimage*, Jun 30 2014.
- [24] N. Leonardi and D. Van De Ville, "On spurious and real fluctuations of dynamic functional connectivity during rest," *Neuroimage*, vol. 104, pp. 430-436, Jan 1 2015.
- [25] T. Adalı, M. Anderson, and G. Fu, "Diversity in independent component and vector analyses: Identifiability, algorithms, and applications in medical imaging," *IEEE Signal Processing Magazine*, vol. 31, pp. 18-33, May 2014.
- [26] N. Leonardi, W. R. Shirer, M. D. Greicius, and D. Van De Ville, "Disentangling dynamic networks: Separated and joint expressions of functional connectivity patterns in time," *Hum Brain Mapp*, Jul 31 2014.
- [27] N. J. Kopell, H. J. Gritton, M. A. Whittington, and M. A. Kramer, "Beyond the Connectome: The Dynome," *Neuron*, vol. 83, pp. 1319-1328, Sep 17 2014, 4169213.
- [28] E. Tagliazucchi and H. Laufs, "Decoding wakefulness levels from typical fMRI resting-state data reveals reliable drifts between wakefulness and sleep," *Neuron*, vol. 82, pp. 695-708, May 7 2014.
- [29] E. Damaraju, E. A. Allen, A. Belger, J. M. Ford, S. McEwen, D. H. Mathalon, B. A. Mueller, G. D. Pearlson, S. G. Potkin, A. Preda, J. A. Turner, J. G. Vaidya, T. G. van Erp, and V. D. Calhoun, "Dynamic functional connectivity analysis reveals transient states of dysconnectivity in schizophrenia," *Neuroimage Clin*, vol. 5, pp. 298-308, 2014, 4141977.
- [30] E. Allen, E. Damaraju, S. M. Plis, E. Erhardt, T. Eichele, and V. D. Calhoun, "Tracking whole-brain connectivity dynamics in the resting state," *Cereb Cortex*, vol. 24, pp. 663-676, 2014, PMC3920766.
- [31] M. Yaesoubi, R. Miller, and V. D. Calhoun, "Dynamic coherence analysis of rest fMRI with state specific phase, frequency and temporal profile," in *Annual Meeting of the Organization for Human Brain Mapping*, Honolulu, HI, 2015.
- [32] N. Leonardi, J. Richiardi, M. Gschwind, S. Simioni, J. M. Annoni, M. Schluep, P. Vuilleumier, and D. Van De Ville, "Principal components of functional connectivity: a new

- approach to study dynamic brain connectivity during rest," *Neuroimage*, vol. 83, pp. 937-950, Dec 2013.
- [33] R. Miller, M. Yaesoubi, and V. D. Calhoun, "Meta-state analysis reveals reduced resting fMRI connectivity dynamism in schizophrenia across multiple multivariate analytic techniques," in *Biennial Conference on Resting State / Brain Connectivity* Boston, MA, 2014.
- [34] M. Yaesoubi, R. Miller, and V. D. Calhoun, "Mutually temporally independent connectivity patterns: A new framework to study resting state brain dynamics with application to explain group difference based on gender," *NeuroImage*, in press, PMC Journal - In Process.
- [35] B. Rashid, E. Damaraju, G. D. Pearlson, and V. D. Calhoun, "Dynamic connectivity states estimated from resting fMRI Identify differences among Schizophrenia, bipolar disorder, and healthy control subjects," *Front Hum Neurosci*, vol. 8, p. 897, Nov 7 2014, 4224100.
- [36] R. C. Craddock, G. A. James, P. E. Holtzheimer, 3rd, X. P. Hu, and H. S. Mayberg, "A whole brain fMRI atlas generated via spatially constrained spectral clustering," *Hum Brain Mapp*, vol. 33, pp. 1914-1928, Aug 2012.
- [37] V. D. Calhoun and T. Adalı, "Multi-subject Independent Component Analysis of fMRI: A Decade of Intrinsic Networks, Default Mode, and Neurodiagnostic Discovery," *IEEE Reviews in Biomedical Engineering*, vol. 5, pp. 60-73, 2012, PMC23231989.
- [38] Q. Lin, J. Liu, Y. Zheng, H. Liang, and V. D. Calhoun, "Semi-blind Spatial ICA of fMRI Using Spatial Constraints," *Hum. Brain Map.*, vol. 31, pp. 1076-1088, 2010, PMC pending #164327.
- [39] E. Acar and B. Yener, "Unsupervised multiway data analysis: A literature survey," *IEEE Trans. Knowl. Data Eng.*, vol. 21, pp. 6-20, 2009.
- [40] A. Y. Mutlu, E. Bernat, and S. Aviyente, "A signal-processing-based approach to time-varying graph analysis for dynamic brain network identification," *Comput Math Methods Med*, vol. 2012, p. 451516, 2012, 3427740.
- [41] D. M. Zoltowski, E. M. Bernat, and S. Aviyente, "A graph theoretic approach to dynamic functional connectivity tracking and network state identification," *Conf Proc IEEE Eng Med Biol Soc*, vol. 2014, pp. 6004-6007, 2014.
- [42] S. Ma, V. D. Calhoun, R. Phlypo, and T. Adalı, "Dynamic changes of spatial functional network connectivity in healthy individuals and schizophrenia patients using independent vector analysis.," *NeuroImage*, vol. 90, 2014, PMC Journal - In Process.
- [43] P. Comon and C. Jutten, *Handbook of Blind Source Separation, Independent Component Analysis and Applications*: Academic Press, Oxford UK, Burlington USA, 2010.
- [44] J. V. Stone, J. Porrill, C. Buchel, and K. Friston, "Spatial, Temporal, and Spatiotemporal Independent Component Analysis of fMRI Data," in *Proc. Leeds Statistical Research Workshop*, Leed, UK, 1999, pp. 1-4.
- [45] V. D. Calhoun, T. Adalı, G. D. Pearlson, and J. J. Pekar, "Spatial and temporal independent component analysis of functional MRI data containing a pair of task-related waveforms," *Hum. Brain Map.*, vol. 13, pp. 43-53, 2001.
- [46] M. J. McKeown and T. J. Sejnowski, "Independent component analysis of fMRI data: examining the assumptions," *Hum. Brain Map.*, vol. 6, pp. 368-372, 1998.
- [47] V. D. Calhoun, T. Adalı, G. D. Pearlson, and J. J. Pekar, "A Method for Making Group Inferences from Functional MRI Data Using Independent Component Analysis," *Human Brain Mapping*, vol. 14, pp. 140-151, 2001.

- [48] E. B. Erhardt, S. Rachakonda, E. J. Bedrick, E. A. Allen, T. Adali, and V. D. Calhoun, "Comparison of multi-subject ICA methods for analysis of fMRI data," *Hum Brain Mapp*, vol. 32, pp. 2075-2095, Dec 2011, 3117074.
- [49] E. Seifritz, F. Esposito, F. Hennel, H. Mustovic, J. g. Neuhoff, D. Bilecen, G. Tedeschi, K. Scheffler, and F. D. Salle, "Spatiotemporal Pattern of Neural Processing in the Human Auditory Cortex," *Science*, vol. 297, pp. 1706-1708, 2002.
- [50] J. H. Lee, T. W. Lee, F. A. Jolesz, and S. S. Yoo, "Independent vector analysis (IVA): multivariate approach for fMRI group study," *Neuroimage*, vol. 40, pp. 86-109, Mar 1 2008.
- [51] R. M. Hutchison, T. Womelsdorf, J. S. Gati, S. Everling, and R. S. Menon, "Resting-state networks show dynamic functional connectivity in awake humans and anesthetized macaques," *Hum Brain Mapp*, vol. 34, pp. 2154-2177, Mar 22 2012.
- [52] A. Zalesky and M. Breakspear, "Towards a statistical test for functional connectivity dynamics," *Neuroimage*, vol. 114, pp. 466-470, Jul 1 2015.
- [53] R. Meyer and N. Christensen, "Bayesian reconstruction of chaotic dynamical systems," *Phys Rev E Stat Phys Plasmas Fluids Relat Interdiscip Topics*, vol. 62, pp. 3535-3542, Sep 2000.
- [54] R. Miller and V. Calhoun, "Data fusion for multimodal multi-feature brain data using Markov-style dynamics in a feature meta-space," in *Pattern Recognition for NeuroImaging (PRNI)*, Palo Alto, CA, 2015.
- [55] R. Miller and V. D. Calhoun, "Meta-state analysis reveals reduced resting fMRI connectivity dynamism in schizophrenia, with dynamic fluidity and range further suppressed by many individual symptoms," in *Society for Neuroscience*, Washington, D. C., 2014.
- [56] M. Yaesoubi, E. A. Allen, R. Miller, and V. D. Calhoun, "Dynamic coherence analysis of resting fMRI data to jointly capture state-based phase, frequency, and time-domain information," *NeuroImage*, in press, PMC Journal - In Process.
- [57] E. Allen, E. Damaraju, S. M. Plis, E. Erhardt, T. Eichele, and V. D. Calhoun, "Tracking whole-brain connectivity dynamics in the resting-state," in *Proc. HBM*, Beijing, China, 2012.
- [58] E. Tagliazucchi, R. Carhart-Harris, R. Leech, D. Nutt, and D. R. Chialvo, "Enhanced repertoire of brain dynamical states during the psychedelic experience," *Hum Brain Mapp*, Jul 3 2014.
- [59] A. Kucyi and K. D. Davis, "Dynamic functional connectivity of the default mode network tracks daydreaming," *Neuroimage*, Jun 25 2014.
- [60] U. Sakoglu, A. Michael, and V. D. Calhoun, "Classification of schizophrenia patients vs healthy controls based on dynamic functional network connectivity," in *Proc. HBM*, San Francisco, CA, 2009.
- [61] J. Gonzalez-Castillo, Z. S. Saad, D. A. Handwerker, S. J. Inati, N. Brenowitz, and P. A. Bandettini, "Whole-brain, time-locked activation with simple tasks revealed using massive averaging and model-free analysis," *Proc Natl Acad Sci U S A*, vol. 109, pp. 5487-5492, Apr 3 2012, 3325687.
- [62] L. Wu, T. Eichele, and V. D. Calhoun, "Reactivity of hemodynamic responses and functional connectivity to different states of alpha synchrony: a concurrent EEG-fMRI study," *NeuroImage*, vol. 52, pp. 1252-1260, 2010, PMC pending #248905.
- [63] D. A. Bridwell, L. Wu, T. Eichele, and V. D. Calhoun, "The spatio-spectral characterization of brain networks: fusing concurrent EEG spectra and fMRI maps," *NeuroImage*, vol. 69, pp. 101-111, 2013, PMC3568990.
- [64] E. Allen, T. Eichele, L. Wu, and V. D. Calhoun, "EEG Signature of Functional Connectivity States," in *Proc HBM*, Seattle, WA, 2013.

- [65] M. E. Raichle, A. M. MacLeod, A. Z. Snyder, W. J. Powers, D. A. Gusnard, and G. L. Shulman, "A default mode of brain function," *Proc.Natl.Acad.Sci.U.S.A*, vol. 98, pp. 676-682, 2001.
- [66] L. Wu and V. D. Calhoun, "An Approach for Fusion between EEG and fMRI Data," in *Proc.ISMRM*, Toronto, Canada, 2008.
- [67] T. Eichele, V. D. Calhoun, and S. Debener, "Mining EEG-fMRI using independent component analysis," *Int. J. Psych.*, vol. 73, pp. 53-61, 2009, PMC2693483.
- [68] T. Deneux and O. Faugeras, "EEG-fMRI fusion of paradigm-free activity using Kalman filtering," *Neural Comput*, vol. 22, pp. 906-948, Apr 2010.
- [69] M. Luessi, S. D. Babacan, R. Molina, J. R. Booth, and A. K. Katsaggelos, "Bayesian symmetrical EEG/fMRI fusion with spatially adaptive priors," *Neuroimage*, vol. 55, pp. 113-132, Mar 1 2011, 3037417.
- [70] D. A. Handwerker, V. Roopchansingh, J. Gonzalez-Castillo, and P. A. Bandettini, "Periodic changes in fMRI connectivity," *Neuroimage*, vol. 63, pp. 1712-1719, Nov 15 2012.
- [71] E. Tagliazucchi and H. Laufs, "Multimodal imaging of dynamic functional connectivity," *Front Neurol*, vol. 6, p. 10, 2015, 4329798.
- [72] E. Tagliazucchi, F. von Wegner, A. Morzelewski, V. Brodbeck, K. Jahnke, and H. Laufs, "Breakdown of long-range temporal dependence in default mode and attention networks during deep sleep," *Proc Natl Acad Sci U S A*, vol. 110, pp. 15419-15424, Sep 17 2013, 3780893.
- [73] E. Damaraju, E. Tagliazucchi, H. Laufs, and V. D. Calhoun, "Dynamic functional network connectivity from rest to sleep," in *OHBM*, Honolulu, HI, 2015.
- [74] J. Gonzalez-Castillo, C. W. Hoy, D. A. Handwerker, M. E. Robinson, L. C. Buchanan, Z. S. Saad, and P. A. Bandettini, "Tracking ongoing cognition in individuals using brief, whole-brain functional connectivity patterns," *Proc Natl Acad Sci U S A*, vol. 112, pp. 8762-8767, Jul 14 2015.

Figure 1: (a) The Chronnectome concept of studying connectivity at multiple time scales⁴, (b) overview of some of the key steps and options used in computing time-varying connectivity measures.

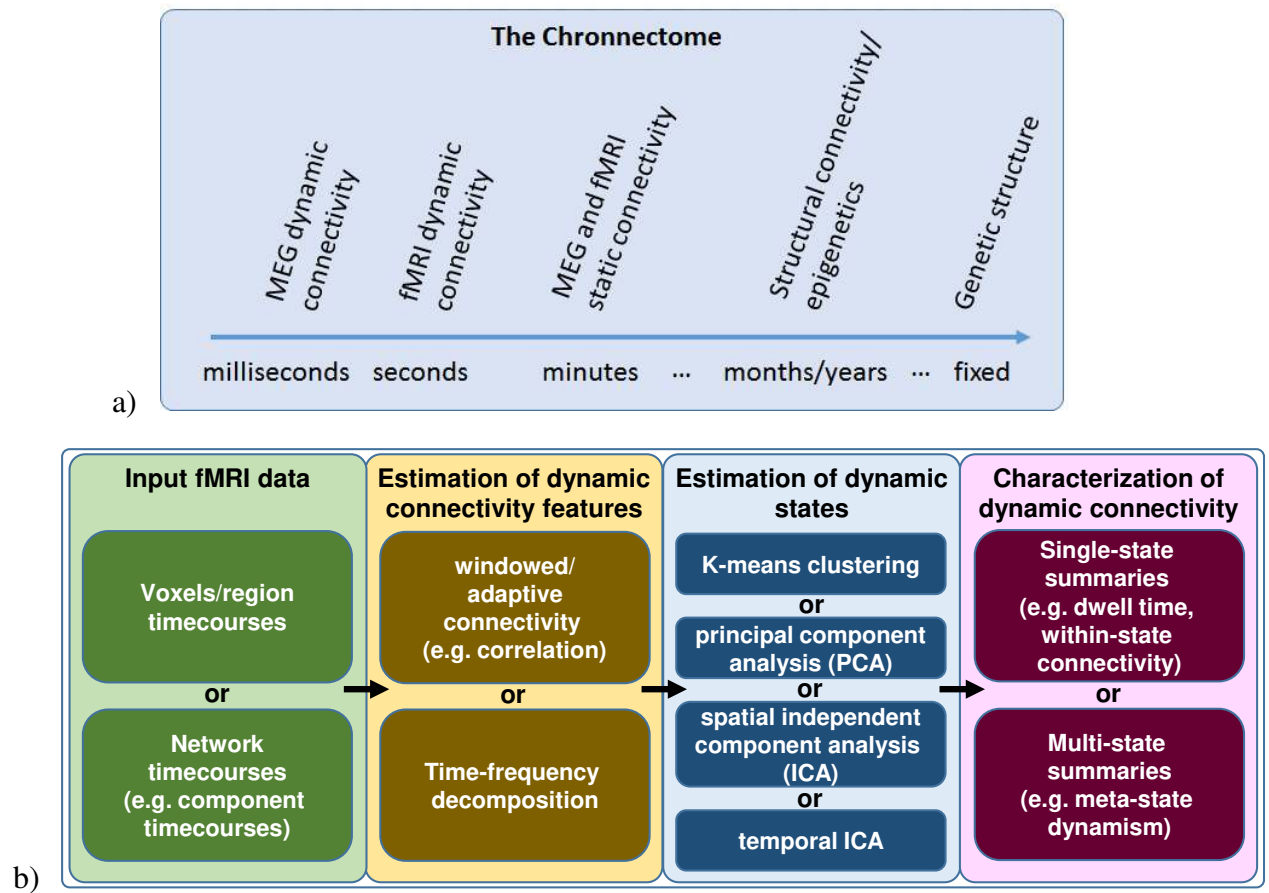


Figure 2: Data-driven maps from group ICA provides components that capture information about within network (component) connectivity that are characterized by timecourses that can be used to assess functional network connectivity (FNC) or among network connectivity which can be assessed in the simplest manner by computing the cross-correlation among component timecourses

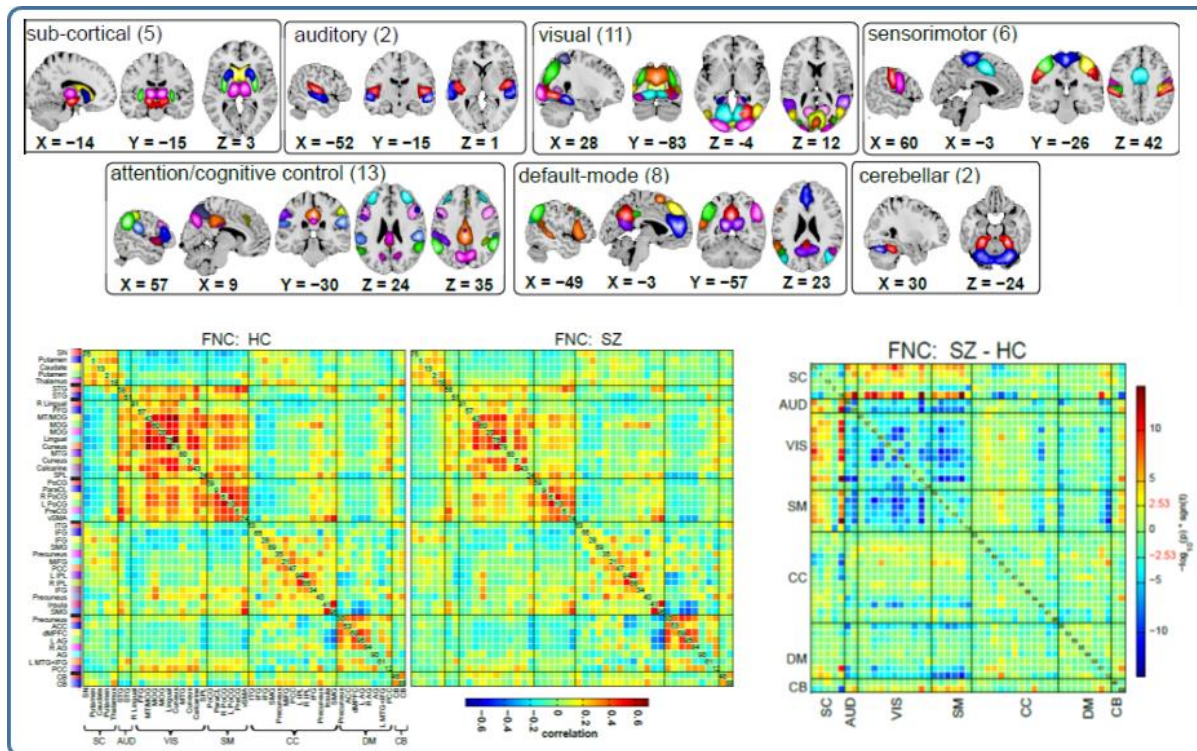


Figure 3: FNC dynamics via windowing: single example subject: (A1) average FNC (cross-correlation of ICA time courses) for a single subject, (A2) FNC time series between select components and snapshots of whole-brain FC30.

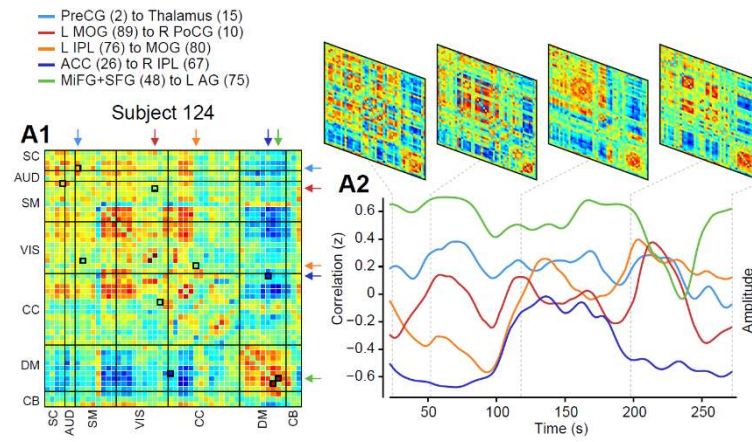


Figure 4: Independent vector analysis approach to characterize spatially dynamic and static components^{4,18,42}. Here spatial maps of a component vector are related over the time windows but should be distinct from the spatial maps of all other components (whether within or outside the current window w_i).

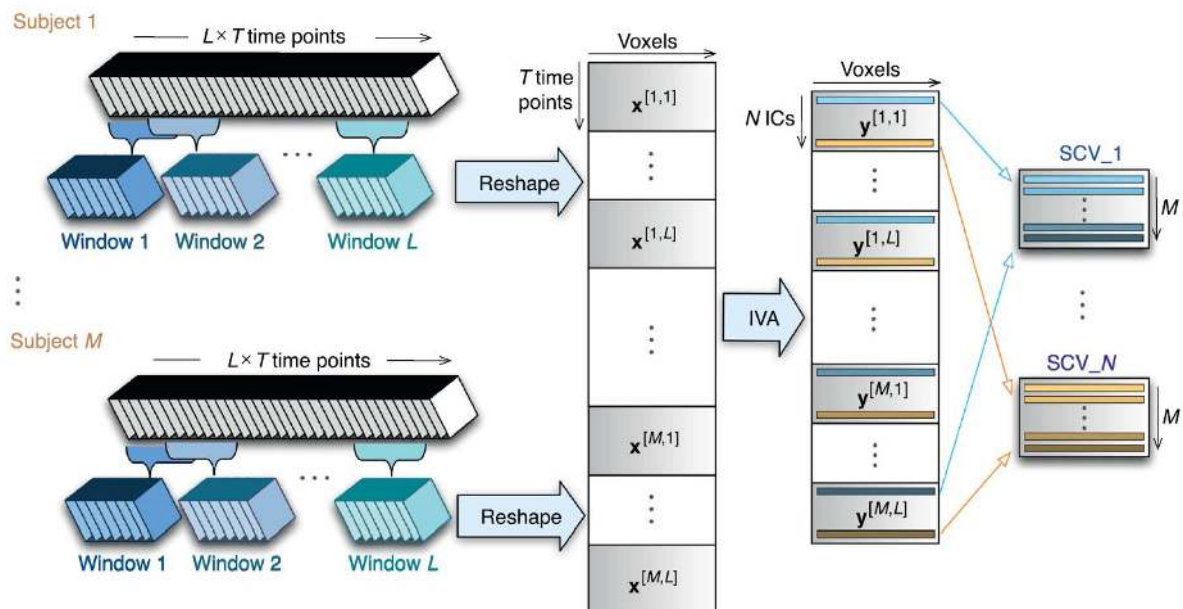


Figure 5: A) State vectors for the three example subjects. Assigned states are plotted at the time point corresponding to the center of the sliding window. (B) The state transition matrix (TM), averaged over subjects. High values along the diagonal indicate a high probability of staying in a state. Note that transition probability is color-mapped on a log-scale. (C) The stationary probability vector (π , principal eigenvector of the TM) shows the steady-state, or “long-run” behavior. Error bars indicate the non-parametric 95% confidence intervals (CIs) obtained from 1000 bootstrap resamples of the average TM (resampling subjects).

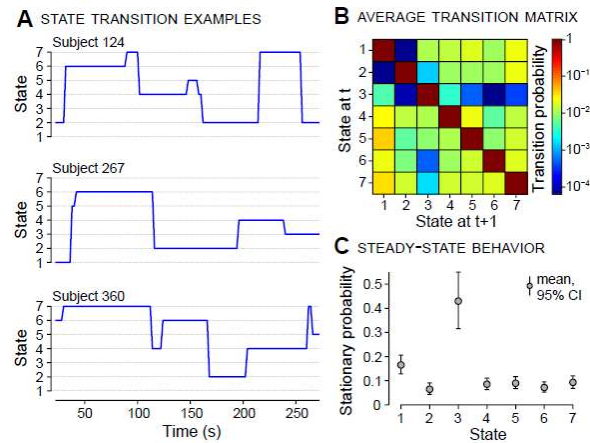


Figure 6: Bar chart shows relative occurrence frequency of each combo-state. The bottom label of each bar is the coded and visual representation of the associated combo-state and the top is labeled by the gender that on average occupies that combo-state more along with the FDR-adjusted p-values for that comparison (dark blue: M>F and dark red: F>M). On the top right corner of the figure, each of the pie chart shows overall occurrence frequency of the associated combo-state³⁴.

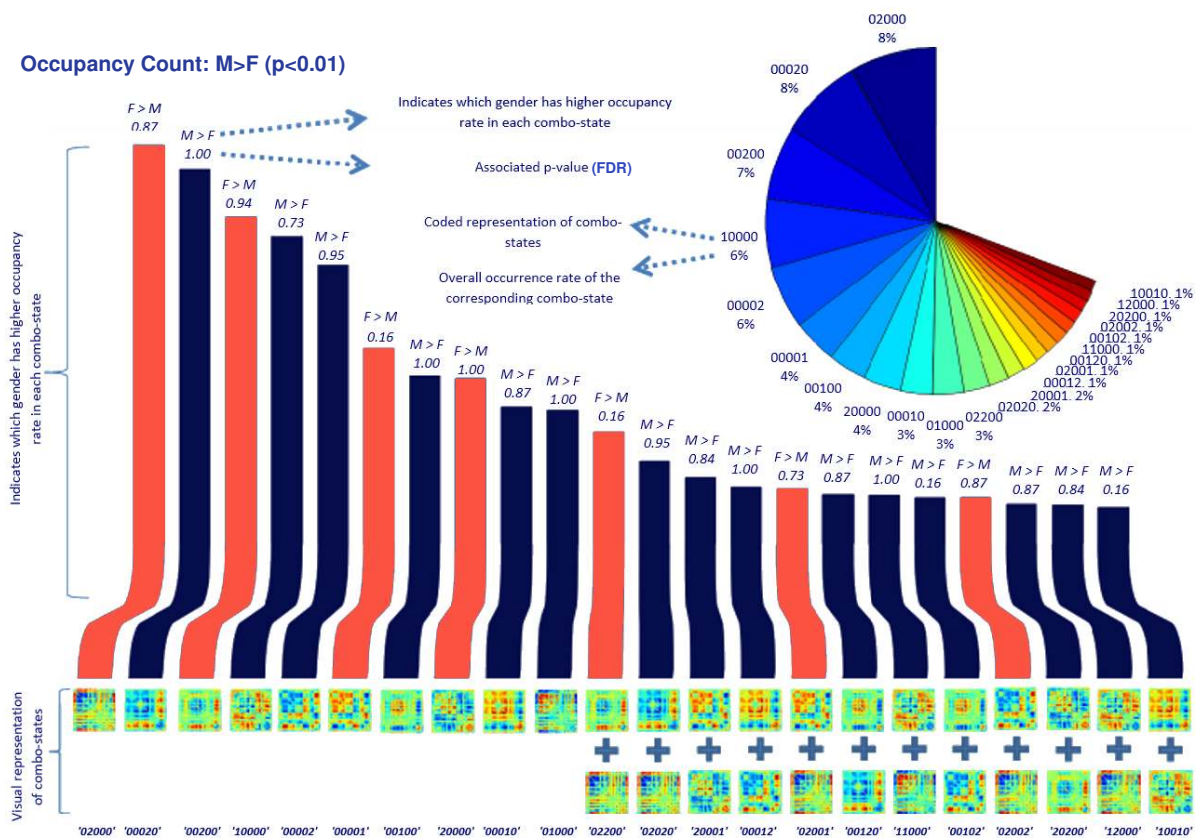


Figure 7: Multiband state with 25% occurrence rate showing the most power in the 0.07 and 0.13 frequency bands. Phase histogram and color indicate the phase of the dynamics.

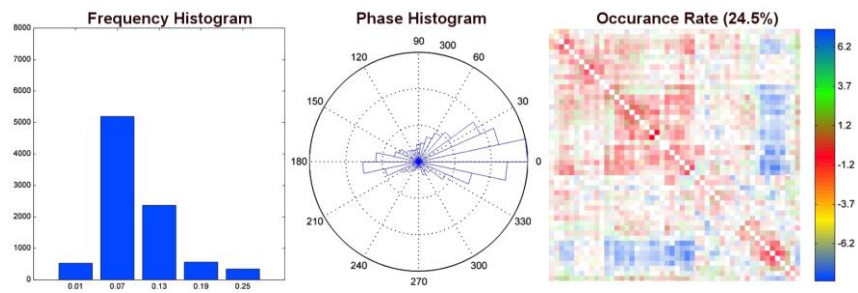


Figure 8: Concurrent EEG/fMRI temporal dynamics during eyes open (EO) versus eyes closed (EC)64. fMRI analysis on the left, and EEG data analyzed within identified fMRI states for one electrode shown on the right top panel. EEG data reflected considerably more theta/delta power during the states occurring more in the EC condition. EEG was strongly correlated with the identified fMRI states as show in the panel on bottom right showing the distance among EEG and fMRI which reduced as EEG windows were shifted in time away from the fMRI states.

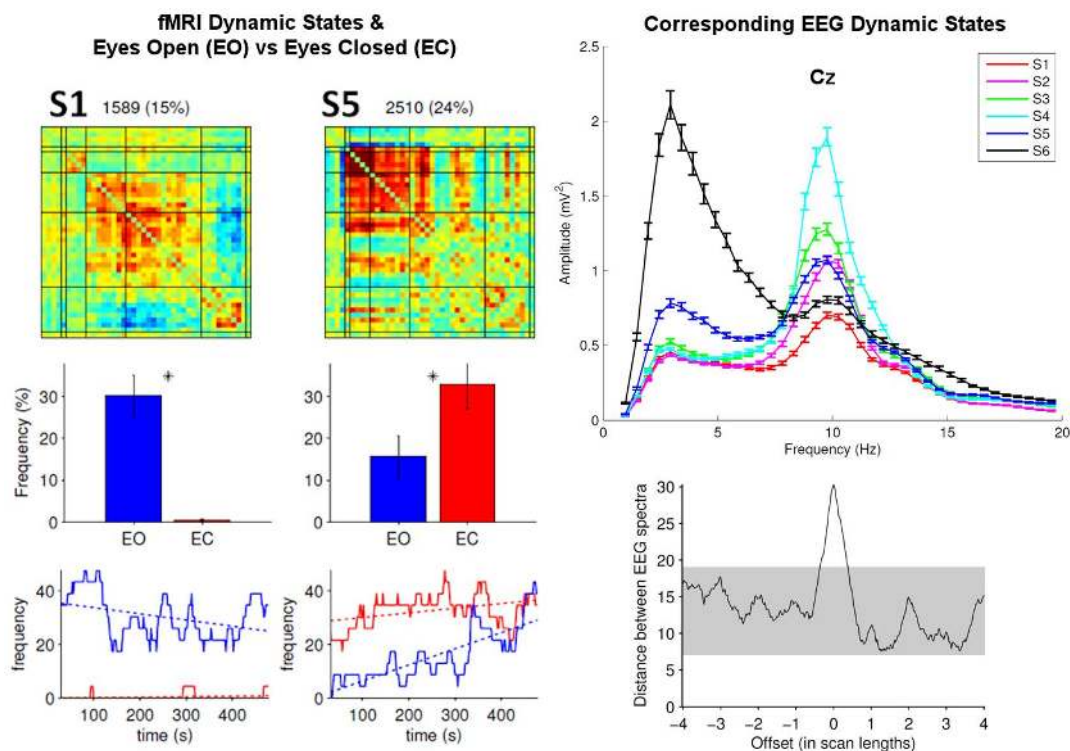


Figure 9: Data showing static FNC pattern estimated by a model incorporating dynamics has higher contrast-to-noise than one ignoring dynamics.

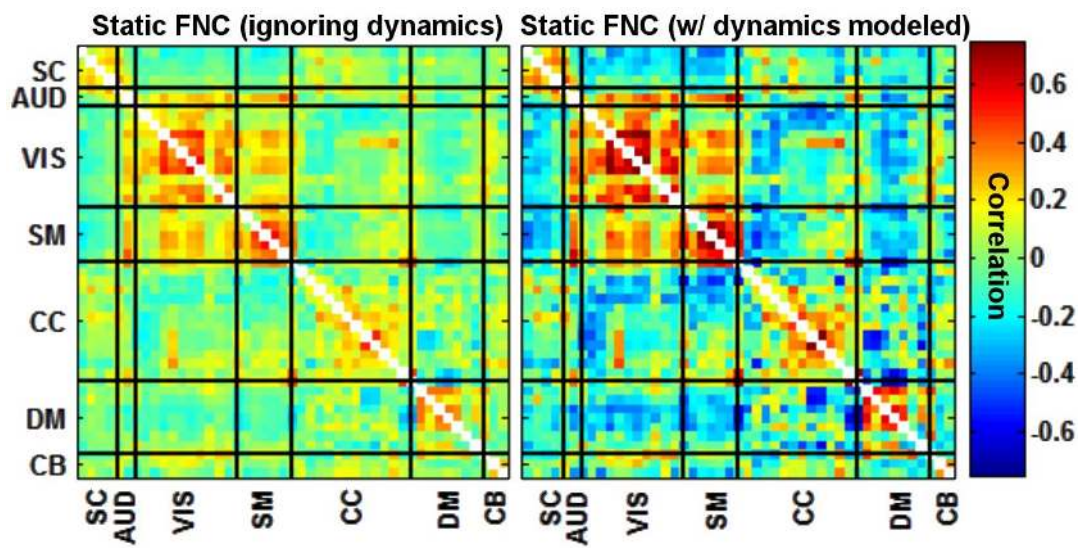


Figure 10: Schizophrenia patients exhibit significant changes in the spatial dependency between default mode and temporal lobe networks.

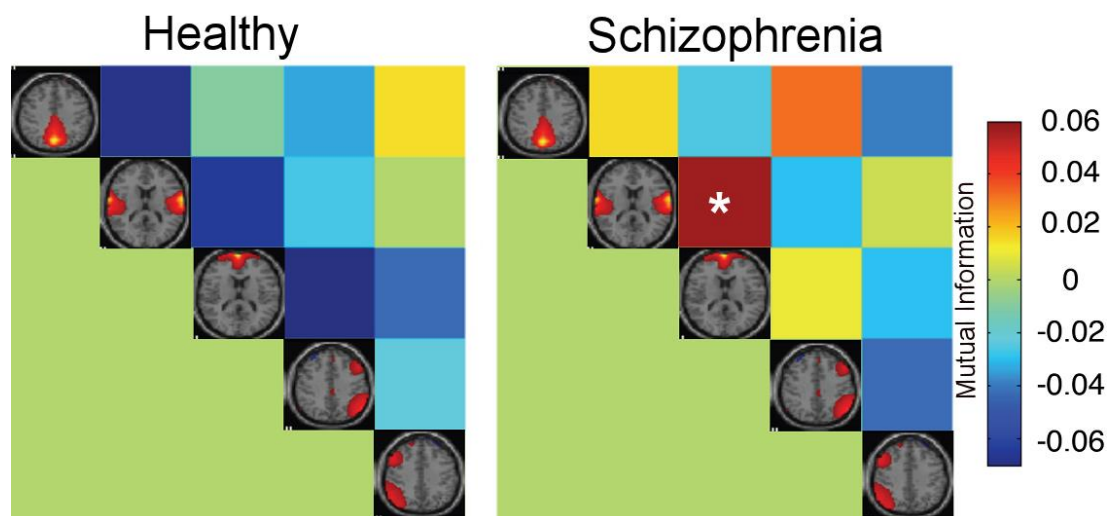


Figure 11: Dynamic states 1 and 5 map onto awake and deeper sleep stages.

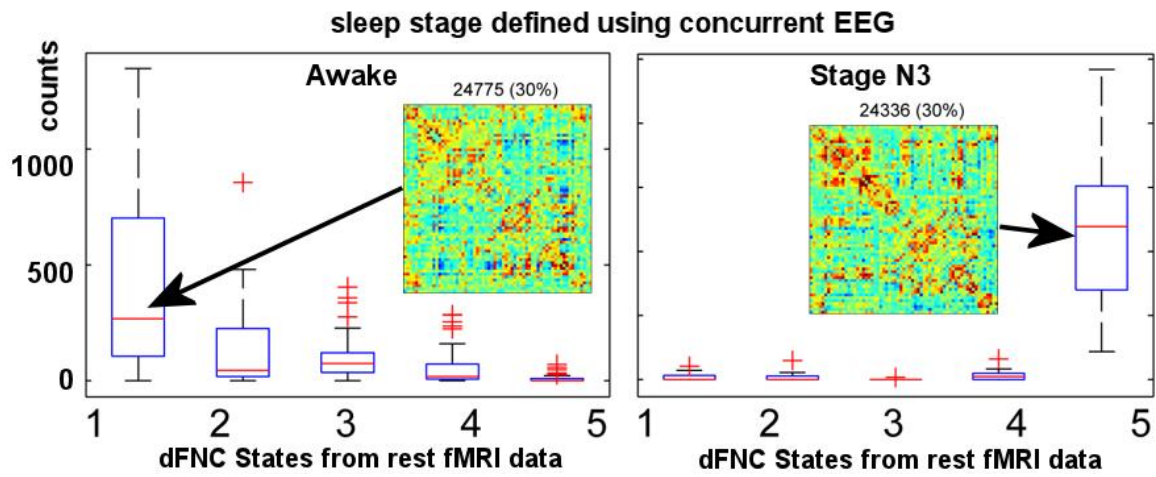


Figure 12: Dynamic FNC ‘states’ that showed significant group differences. In particular, smoker and drinker spent more time in State 1 vs State 2 (of 5 estimated states). Notably, state 1 lacks the predominant anticorrelation between default mode regions which is visible in state 2 suggesting their lack may serve as either a protective factor or as a marker of substance use.

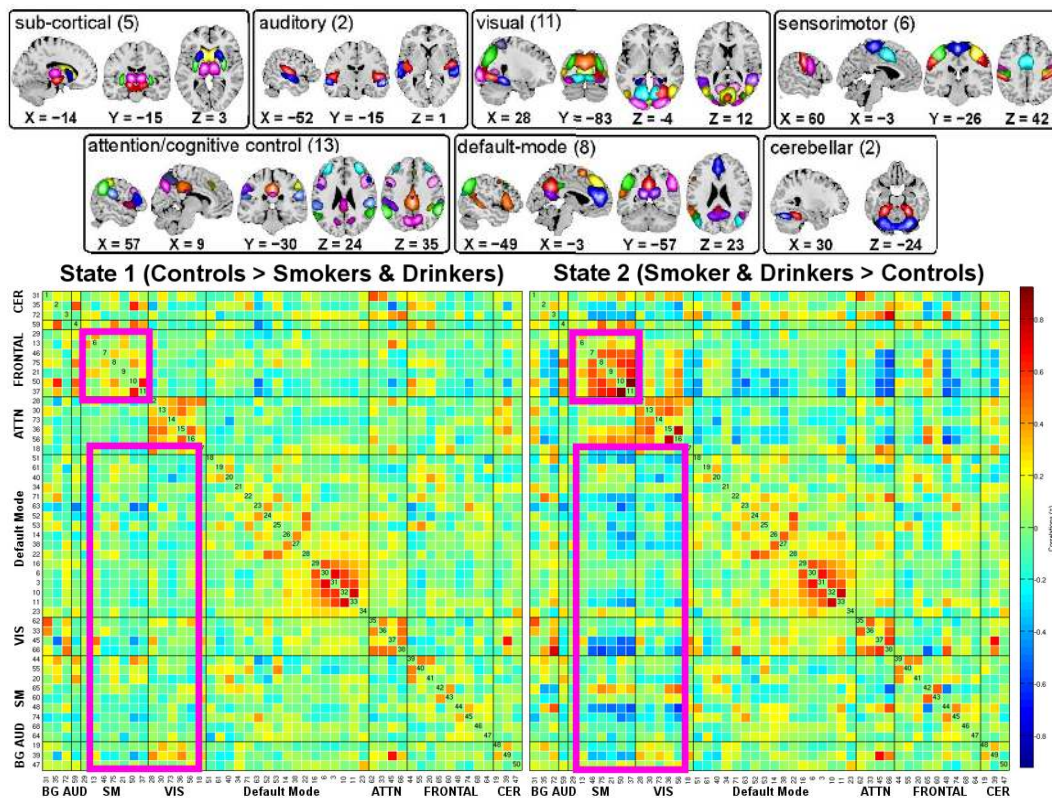


Figure 13: Dwell time (percent) for states 1 and 2. Smoker and drinkers are spending significantly ($p < 0.0001$) more time in state one whereas controls are spending more of their time in state 2.

